MULTIPLE LABELS POINT-SET REGISTRATION

Eric Van Reeth[1]*, Michael Sdika*[1]*, Pierre-Hervé Luppi*[2]*, Paul-Antoine Libourel*[2]*, Olivier Beuf*[1]

[1]Université de Lyon, CREATIS; CNRS UMR5220;
Inserm U1044; INSA-Lyon; Université Lyon 1, France.
[2]Centre de Recherche en Neurosciences de Lyon; Inserm U1028 - CNRS UMR5292

ABSTRACT

A multi-label point-set registration method is presented in this paper. It focuses on carefully computing an initial transform to help the registration process converge towards the optimal deformation. The proposed method is particularly efficient in cases where the deformation is discontinuous or nearly discontinuous. A simple synthetic example is presented to illustrate the advantage of the method. A real-data example is also presented in the context of multi-modality registration (blockface to Magnetic Resonance Imaging, MRI) for brain atlas construction. In both examples, visual and numeric results illustrate the superiority of the presented method compared to two recent multi-label registration contributions.

***Index Terms*—** Point-set registration, Deformable registration, Rigidity constraints, Atlas construction, Tupinambis

1. INTRODUCTION

Point-set registration consists of estimating the transformation between segmented structures, represented as point-sets. This is an important step in medical image applications where the deformation between structures needs to be evaluated, as for example in the atlas construction problem [1]. Various approaches have been tested for point-set registration. A classical approach is the iterative closest point (ICP) [2], which iteratively derives the optimal transform that matches the correspondence between the fixed and moving point-sets. Several implementations of this method are compared and reviewed in [3]. Landmark matching has also been used in the context of point-set registration, based on the work of Bookstein [4] where thin-plate splines are used to interpolate the deformation between non-uniformly scattered fixed and moving landmarks. More recently, an other set of approaches based on information theory was investigated to measure the disparity between point-sets probability density functions (PDF), generally derived from Gaussian mixture models. Several distances between point-set PDF have been investigated in the literature to optimize the registration process. Jian and Vermuri use a $\mathcal{L}_2$ distance [5], while Wang et al. propose the Jensen-Shannon divergence as an efficient and unbiased distance in the context of atlas construction [1]. Pluta et al. implemented a Point-Set-Expectation method (PSE) based on a bi-directional expected matching term between structures to be registered. It minimizes the distance between each point of a given point-set and the expected corresponding point from the other point-set. More recently, Tustison et al. introduced the Jensen–Havrda–Charvat–Tsallis (JHCT) divergence as a point-set PDF distance [6]. Their formalism allows the registration of multi-label point-sets by minimizing a cost function defined as the sum on all labels of the JHCT divergence for all point-sets.

All these methods might find a local minimum to the registration process, since nothing is done to improve the robustness or attempt to avoid local minima using the specificity of the multi-labels point set registration problem. More specifically, the registration might be driven by the largest structures or the one requiring more deformation, which may be done to the detriment of other structures. If the deformations significantly differ from one label to an other, discontinuities might appear in the global transform which makes it hard to recover. Such discontinuities are present in real life problem when structures that are far apart in one image are adjoin in another. This frequently happens when registering in-vivo to ex-vivo images such as MRI to blockface or histology, as illustrated in Figure 1.

This paper tackles the problem of finding a correct initialization to the point-set registration in order to facilitate the convergence towards the global optimum. Both synthetic and real data examples illustrate the impact of the proposed initialization when compared to recent state-of-the art methods.

2. METHODS

The concept of our method can be split into three steps. First, all moving labels are independently registered to the corresponding fixed labels to define one transform T_k for each label. Then, a transform $T_s(x)$ which is close to each T_k on the mask of the k-th label is estimated. Finally, T_s is used as an

This work was founded by the "Avenir Lyon Saint-Etienne" program from the Université de Lyon in the framework of the "Investissements d'Avenir" (ANR-11-IDEX-0007) operated by the French National Research Agency (ANR).

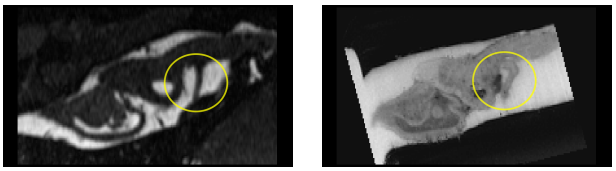

(a) MRI (b) Blockface

Fig. 1: Illustration of an in-vivo to ex-vivo deformation on the Tupinambis brain.

initialization of a final registration process including all labels in the metric, allowing to efficiently avoid local minima and potentially reduce the required number of iterations.

2.1. Independent label registration

Let us here define T_k, the deformation between the fixed image k-th label : $M_k^f(x)$, and the moving image k-th label : $M_k^m(x)$. It is assumed in this paper that all T_k deformations are deformable, but advantages of the proposed method still hold for affine or rigid deformations. Each T_k is computed as a composition of an affine and a B-spline transform, by minimizing the sum of square difference of the signed distance transforms (SDT) of $M_k^f(x)$ and $M_k^m(x)$. The SDT image $D_k^f(x)$ is the image of the Euclidean distance of x to the boundary of the label k. It is positive outside Ω_k and negative inside. $D_m^f(x)$ are defined similarly for the labels of the moving image. SDT was used for geometrical shapes registration in [7]. Its main advantage in our context is that it facilitates registration of labels that initially have a poor spatial correspondence, since all voxels give an indication about the distance to the object to be matched. Each T_k is obtained by firstly computing the affine component (T_a), and secondly the B-spline (T_b) transform as:

$$T_k = \underset{T\in\mathcal{D}_T}{\arg\min} \sum_{x\in\Omega_I} \|D_k^m(T(x)) - D_k^f(x)\|^2$$

with $T(x) = T_b \circ T_a(x)$, Ω_I the spatial support of the image and $\mathcal{D}_T$ the domain where the transform belong. $\mathcal{D}_T$ can, for example, include voxelwise constraints such as in [8] or be defined using the flow of diffeomorphism formalism of [9]. Note that attributing a label to the background and registering it in the same way as the other labels might improve the final registration. Note also that our implementation based on a least square registration of the SDT can be replaced by any deformable registration of binary shapes such as [1, 6].

2.2. Computing T_s

The next step consists of merging the independent registrations into a unique deformable transformation defined on the entire image domain: T_s. Let us first define $\tilde{T}(x) = \sum_{k=1}^K M_k^f(x) T_k(x)$. It is obvious that $\tilde{T}$ contains discontinuities at the border between masks since all T_k are independent, and is thus not invertible. We choose to define T_s as the closest invertible deformable transform to $\tilde{T}$. To do so, we define

$$T_s = \underset{T\in\mathcal{D}_T}{\arg\min} \sum_{x\in\Omega_I} \|T(x) - \tilde{T}(x)\|^2 \quad (1)$$

$$= \underset{T\in\mathcal{D}_T}{\arg\min} \sum_{d} \sum_{x\in\Omega_I} \|I^d(T(x)) - \tilde{T}^d(x)\|^2 \quad (2)$$

where d is the d-th dimension of the image, I^d is the coordinate voxel map in the d-th dimension (i.e. $I^d(x) = x^d$), and $\tilde{T}^d(x) = I^d(\tilde{T}(x))$. As one can see on the equation 2, T_s is the solution of a registration problem: state of the art registration software can be used for its estimation. After convergence, $T_s(x)$ defines a global transform that approximates $\tilde{T}$ in all dimensions. Regularity constraints can be added in order to regulate the degrees of freedom allowed to T_s, and ensure its invertibility [10]. On the other hand, adding too much constraints will decrease the quality of the approximation of $\tilde{T}$ and produce a poor initialization. The optimal regularity trade-off depends on the nature of the discontinuities of the registration problem. Note that using this scheme offers a nice flexibility since any type of transform can be chosen to approximate $\tilde{T}$.

2.3. Using T_s as an initialization

Once T_s is defined, it is used to initialize a classical multi-image registration problem to estimate the final transform (T_f) with any chosen metric m as :

$$T_f(x) = \underset{T\in\mathcal{D}_T}{\arg\min} \sum_{k=1}^{N} \sum_{x\in\Omega_I} m(M_k^m(T\circ T_s(x)), M_k^f(x)) \quad (3)$$

Regularity constraints can be added to Eq. 3 to ensure invertibility and include prior information in the registration scheme.

3. RESULTS

In this section, the proposed method will be evaluated and compared with other methods on both synthetic and real data examples. The first method is a naive registration using a B-spline transformation model and a mean-square error (MSE) metric. The B-spline node spacing is set to $(1 \times 1 \times 1)$ pixel in order to allow as much degrees of freedom as possible. The two other methods are the PSE [11] and JHCT [6], implemented in ANTs [12]. They use a symmetric diffeomorphic transformation model. Different values of the regularization smoothness parameter (including 0) are tested to make sure the transformation is not too constrained. The proposed multi-segmentation registration (MSR) method was implemented with Elastix [13]. It uses a B-spline transformation model with the corresponding node spacings: $(8 \times 8 \times 8)$ pixels for T_k, $(1 \times 1 \times 1)$ pixel for T_s and $(8 \times 8 \times 8)$ pixels

	Naïve	PSE [11]	JHCT [6]	MSR
L1	0.979	0.919	0.880	**0.981**
L2	0.983	0.966	0.900	**0.999**

Table 1: Dice coefficients for the synthetic data example

for T_f. All methods were run for a wide range of parameters, and results giving the best average Dice coefficients are kept for comparison.

3.1. Synthetic Example

The synthetic example is illustrated in Fig. 2. Two cubes initially separated by one voxel, are translated in opposite directions which creates a discontinuity in the deformation field. Note that the left cube also deforms to a sphere to challenge the registration process. Fig. 2 illustrates the registration results obtained for all 3 methods. It is clear that all methods except MSR have troubles capturing the discontinuity. It is interesting to notice that although the naive result has more degrees of freedom than the final transform of MSR (T_f) it is unable to produce a correct registration, which illustrates the importance of a correct initialization. The two other methods are not able either to recover the sphere nor the cube correctly close to the discontinuity. Resulting Dice coefficients are given in Table 1.

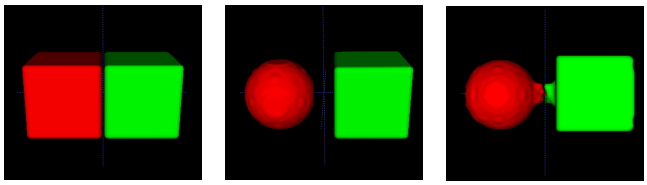

(a) Moving image (b) Fixed image (c) Naive result

(d) JHCT (e) PSE (f) MSR

Fig. 2: Registration results on the synthetic data.

3.2. Real Data Example

All methods have been subsequently tested on a real problem of segmentation based registration of a blockface acquisition to an MRI of the same Tupinambis brain. Two subjects were included in this study. Blockface (BF) is an ex-vivo modality composed of stacked high-resolution 2D photographs of the frozen extracted brain before slicing. Severe deformations (shrinking, tearing) can happen independently on some structures during the brain extraction, the freezing and the slicing process. Performing registration on segmented structures instead of directly working on images can help to compensate

	L1	L2	L3	L4	L5	L6	L7
PSE (S1)	0.66	0.86	0.82	0.86	0.79	0.92	0.94
JHCT (S1)	0.58	0.87	0.77	0.84	0.82	0.94	0.93
MSR (S1)	**0.85**	**0.91**	**0.88**	**0.92**	**0.84**	**0.96**	**0.96**
PSE (S2)	0.64	0.87	0.75	0.81	0.82	0.86	0.86
JHCT (S2)	0.71	0.91	0.65	0.78	0.82	0.94	0.93
MSR (S2)	**0.85**	**0.95**	**0.89**	**0.94**	**0.92**	**0.98**	**0.98**

Table 2: Dice coefficients for the real data example

for such alterations and feed the registration process with an important *a priori*. The resolution of the blockface volume is : $10 \times 10 \times 50\ \mu\text{m}^3$. This volume is subsequently subsampled to match the MRI spatial resolution and 7 structures are segmented as illustrated in Fig. 3 (d).
The MRI acquisition is a FIESTA-C (Fast Imaging Employing Steady sTate Acquisition with phase Cycling) sequence. It is acquired on a 3T MR750 system (GE Healthcare, USA) using a 8-channel wrist array coil at a spatial resolution of : $0.16 \times 0.16 \times 0.2\ \text{mm}^3$. The MRI volume and the associated segmentation are shown on Fig. 3 (a).

Table 2 shows the Dice coefficient results for both subjects (S1 and S2), and Fig. 3 shows the registration results of the compared methods. It is clear both visually and numerically that the MSR method is able to detach structures that were brought together during the brain extraction process - mostly the forebrain (L7, purple), the optic tectum (L4, yellow) and the cerebellum (L1, red).
The proposed initialization allows to use simple metrics and a simple transformation model (B-spline) to model the final transformation (T_f) and still produce satisfactory registration results. As suggested in part 2.3, rigidity constraints were applied to Eq. 3 in order to maintain anatomical coherence of the structures and force invertibility. A significant proportion of the computation time is spent on T_s due to the high number of transform parameters. This is justified by the fact that the deformation is complex and has a high number of discontinuities. Total computation time was around 2 hours and 30 minutes on a quad-core machine at 2.50GHz.

4. CONCLUSION

A multi-label registration that focuses on computing a good initialization was presented in this paper. The initial transform is defined on the entire image domain and approximates, under user-defined constraints, individual label transforms that were previously computed. Significant improvement is achieved when comparing our method to two recent multi-label registration algorithm in the case where the deformation has one or more discontinuities. Starting with a good initialization clearly improves the deformation estimation and might also reduce the required number of iterations for the final estimation. This method was developed in the context of atlas construction where registration accuracy and invertibil-

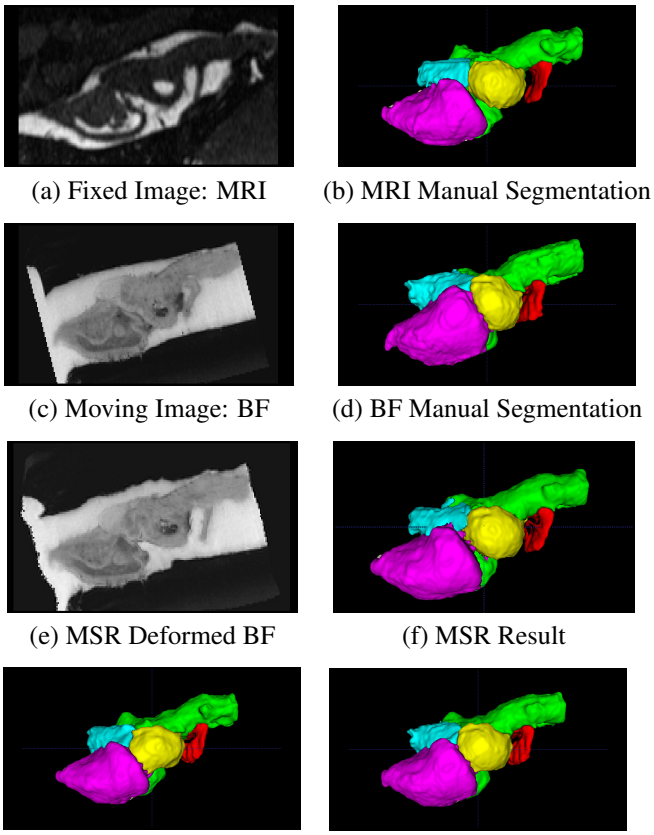

(a) Fixed Image: MRI (b) MRI Manual Segmentation

(c) Moving Image: BF (d) BF Manual Segmentation

(e) MSR Deformed BF (f) MSR Result

(g) JHCT Result (h) PSE Result

Fig. 3: Registration results on the Tupinambis brain data. Best viewed in electronic version.

ity are of prime importance. However, the proposed method is highly flexible and can be adapted to different contexts. The type of transforms chosen for T_k, T_s and T_f, the number of degrees of freedom, and various types of constraints and metrics can be adapted to the application. There is often a compromise to be done between the amount of constraints and the approximation quality by T_s of each T_k. Finally, the method was implemented using Elastix binaries but could be developed under any other framework. Future work will include applying MSR on other Tupinambis subjects, investigating the merging of the T_s and T_f steps and enlarging the scope of tested transforms.

5. REFERENCES

[1] Fei Wang, B C Vemuri, A Rangarajan, and S J Eisenschenk, "Simultaneous Nonrigid Registration of Multiple Point Sets and Atlas Construction," *IEEE Transactions on Pattern Analysis and Machine Intelligence*, vol. 30, no. 11, pp. 2011–2022, Nov. 2008.

[2] Paul J. Besl and Neil D. McKay, "A Method for Registration of 3-D Shapes," *IEEE Transactions on Pattern Analysis and Machine Intelligence*, vol. 14, no. 2, pp. 239–256, 1992.

[3] S. Rusinkiewicz and M. Levoy, "Efficient variants of the ICP algorithm," in *Proceedings Third International Conference on 3-D Digital Imaging and Modeling*. 2001, pp. 145–152, IEEE Comput. Soc.

[4] Fred L Bookstein, "Principal warps: Thin-plate splines and the decomposition of deformations," *IEEE Transactions on Pattern Analysis and Machine Intelligence*, vol. 11, no. 6, pp. 567–585, 1989.

[5] Bing Jian and B C Vemuri, "A robust algorithm for point set registration using mixture of Gaussians," in *Tenth IEEE International Conference on Computer Vision*, Oct. 2005, vol. 2, pp. 1246–1251.

[6] Nicholas J. Tustison, Suyash P. Awate, Gang Song, Tessa S Cook, and James C Gee, "Point set registration using Havrda–Charvat–Tsallis entropy measures," *IEEE Transactions on Medical Imaging*, vol. 30, no. 2, pp. 451–460, 2011.

[7] Nikos Paragios, Mikael Rousson, and Visvanathan Ramesh, "Non-rigid registration using distance functions," *Computer Vision and Image Understanding*, vol. 89, no. 2-3, pp. 142–165, 2003.

[8] Michaël Sdika, "A fast nonrigid image registration with constraints on the Jacobian using large scale constrained optimization," *IEEE Transactions on Medical Imaging*, vol. 27, no. 2, pp. 271–281, 2008.

[9] Alain Trouvé, "Diffeomorphisms Groups and Pattern Matching in Image Analysis," *International Journal of Computer Vision*, vol. 28, no. 3, pp. 213–221, 1998.

[10] Marius Staring, Stefan Klein, and Josien P W Pluim, "A rigidity penalty term for nonrigid registration," *Medical Physics*, vol. 34, no. 11, pp. 4098–4108, 2007.

[11] John Pluta, Brian B Avants, Simon Glynn, Suyash P. Awate, James C Gee, and John A Detre, "Appearance and incomplete label matching for diffeomorphic template based hippocampus segmentation," *Hippocampus*, vol. 19, no. 6, pp. 565–571, 2009.

[12] Brian B Avants, Nick Tustison, and Gang Song, "Advanced Normalization Tools (ANTS)," *Insight Journal*, pp. 1–35, 2011.

[13] Stefan Klein, Marius Staring, Keelin Murphy, Max a Viergever, and Josien P W Pluim, "Elastix: a Toolbox for Intensity-Based Medical Image Registration.," *IEEE Transactions on Medical Imaging*, vol. 29, no. 1, pp. 196–205, Jan. 2010.